

Review and Synthesis of Roughness-Dominated Transition Correlations for Reentry Applications

Daniel C. Reda

NASA Ames Research Center, Moffett Field, California 94035-1000

Nomenclature

a	= constant; Fig. 1
C, C'	= constants
k	= roughness element height, ft
\bar{k}	= average roughness element height, ft
L	= vehicle length, ft
M	= Mach number
n	= exponent; Fig. 1
\bar{R}	= Poll's transition parameter ^{29,30} ; Eq. (1)
Re_{ke}	= roughness Reynolds number based on height k and edge conditions
Re_{kk}	= roughness Reynolds number based on height k and conditions at k
Re_{θ}	= Reynolds number based on height θ and edge conditions
U	= velocity component parallel to test surface or velocity component perpendicular to attachment line, ft/s
V	= velocity component parallel to attachment line, ft/s
X	= generalized disturbance parameter or axial coordinate along windward centerline
x	= coordinate perpendicular to attachment line, ft
Y	= generalized transition parameter
α	= angle of attack, deg
δ	= smooth-wall laminar boundary-layer thickness, ft
η	= Poll's length scale ^{29,30} [Eq. (2)], ft
θ	= smooth-wall laminar boundary-layer momentum thickness, ft
μ	= viscosity, lbm/ft · s
ν	= kinematic viscosity, ft ² /s
ρ	= density, lbm/ft ³

Subscripts

al	= attachment line
e	= edge of smooth-wall laminar boundary layer
k	= based on conditions in smooth-wall laminar boundary layer at top of roughness elements
tr	= transition
w	= wall or based on wall temperature

Superscript

*	= properties evaluated at Poll's reference temperature ^{29,30}
---	-------------------------------------------------------------------------

Introduction

MODELING of roughness-dominated transition is a critical design issue for both ablating and nonablating thermal protection systems (TPS). Ablating TPS, for single-use planetary-entry and Earth-return missions, first experience recession under high-altitude, low-Reynolds-number conditions. Such laminar-flow ablation causes the formation of a distributed surface microroughness pattern characteristic of the TPS material composition and fabrication process. For nonablating TPS, such as the overlapping metallic-panel heatshields proposed for future reusable launch vehicles, the initial distributed surface roughness pattern is established a priori by the engineering design and assembly procedure. However, under high-altitude laminar heating, such metallic panels undergo thermal distortion, causing the formation of a distributed surface roughness pattern of multiple height scales.

In both cases, these distributed surface roughness patterns create disturbances within the laminar boundary layer flowing over the surface. As altitude decreases, Reynolds number increases, and flowfield conditions capable of amplifying these roughness-induced perturbations are eventually achieved, that is, transition onset occurs. Boundary-layer transition to turbulence results in more severe heat transfer rates. Ablating TPS experience increased recession rates, leading to potential burn through, whereas nonablating, metallic-panel TPS experience accelerated temperature rise, leading to potential surface coating failures and melting of components.

The objectives of this paper are 1) to restate the author's earlier conclusions concerning the validity of the critical roughness Reynolds number concept for blunt bodies in hypersonic flow,¹ 2) to reanalyze the roughness-dominated transition correlations published since that time, and 3) to attempt to unify the correlating approach applied to roughness-dominated transition data sets in terms of the physics-based, critical roughness Reynolds number framework. This paper focuses on published roughness-dominated transition correlations, and no attempt was made to cite every roughness-dominated transition data point ever reported.

Important differences between critical roughness Reynolds numbers measured in isolated vs distributed roughness experiments will be emphasized, and the applicability of isolated vs distributed roughness correlations to lifting entry vehicle design will be discussed. The present review paper on roughness-dominated transition, combined with the recent review papers by Schneider on flight-test data²



Daniel C. Reda recently joined the Space Technology Division at NASA Ames Research Center as a Senior Scientist, responsible for aerothermodynamics research to support access-to-space and planetary-entry missions. Previously, he was a Senior Research Scientist in the Ames Research Center Fluid Mechanics Laboratory, where he developed a global surface shear stress vector measurement method using liquid crystal coatings. Before returning to Ames Research Center in 1990, he was a Research Scientist for reentry physics at both the Sandia National Laboratories, Albuquerque, New Mexico, and the U.S. Naval Ordnance Laboratory, White Oak. His Ph.D. was awarded by Rutgers University, and his postdoctoral training was conducted at NASA Ames Research Center under National Research Council funding. Daniel Reda is a Fellow of AIAA and holds patents on aerodynamic measurement technologies. He has served on the AIAA Fluid Dynamics, Thermophysics, and Aerodynamic Measurement Technology Technical Committees.

and noise effects,³ provides a detailed summary of available transition design correlations and databases.

Evolution of Critical Roughness Reynolds Number Correlating Approach

The concept of a critical roughness Reynolds number for transition is attributed to Schiller,⁴ who hypothesized that, at some critical value, vortices would be shed from the top of the roughness element(s), causing an abrupt breakdown to turbulence. The critical Reynolds number was based on smooth-wall laminar boundary-layer conditions at the roughness height, and the length scale was the roughness height. Early experimental research on roughness-dominated transition and the evolution of the critical roughness Reynolds number concept are documented in Refs. 5–15 and references given therein.

For isolated (single) roughness elements, breakdown to turbulence was generally first observed downstream of the element, but with small additional increases in freestream unit Reynolds number, the turbulent wedge would flash forward and become attached to the element. The trip was then defined as effective. The value of the critical roughness Reynolds number was dependent on roughness element height, shape, type (two or three dimensional) and flow-field, for example, incompressible, flat plate. No universal value was discovered in these early experiments.

For three-dimensional distributed roughness elements covering the entire test surface, the term effective tripping was replaced by critical roughness Reynolds number for the onset of turbulence, which occurred at the axial location along the test surface where the critical value was first achieved. This location was typically defined as the location where an abrupt rise in the wall temperature, or wall heat flux, above the local laminar value, was measured. In a time-varying flowfield, the transition front would progress (move) over the rough surface consistent with the physical location where the critical value was locally achieved.

Reshotko and Leventhal,¹⁶ Reshotko,¹⁷ and Tadjfar et al.¹⁸ conducted detailed experiments in the early 1980s on instabilities within, and the breakdown of, laminar boundary layers flowing over three-dimensional distributed surface roughness patterns. Results corroborated the critical roughness Reynolds number concept as outlined by Schiller.⁴ According to Reshotko,¹⁷ “the departure from laminar flow is explosive and related to effects occurring in the near vicinity of the roughness (peaks).” From Ref. 18, “Near the beginning of transition, a single frequency oscillation was measured in both streamwise and vertical velocity fluctuations. While maintaining the same narrow band frequency content, this oscillation amplified rapidly as it moved downstream.” Furthermore, “The single frequency oscillation measured could be attributed to shedding of (these) hairpin vortices.” Also, “The contributions of the downstream roughness elements would thus increase the strength of the vortices toward the eventual transition.” Present understanding indicates that distributed surface roughness patterns promote earlier transition to turbulence when compared to the tripping effectiveness of a single roughness element of equivalent height and shape.

As will be seen in subsequent sections, this simple physical model for vortex shedding/breakdown to turbulence successfully describes roughness-dominated transition for incompressible and compressible flows, over isolated and distributed roughness elements, for blunt-body, attachment-line, and lifting-entry vehicle geometries. The value of the critical roughness Reynolds number for any flow-field/roughness pattern combination must be determined empirically in a quiet ground-based test facility or in-flight.

Nosetips

By the mid-1970s, cold war concerns had generated extreme interest in transition physics on ablating nosetips of ballistic reentry vehicles.^{19,20} Under the Passive Nosetip Technology (PANT) program,²¹ a substantial new database for roughness-dominated transition on blunt bodies in hypersonic flow was generated. Metallic models with uniform, three-dimensional, distributed surface roughness patterns, of parametrically varied height scales, were systematically tested in conventional (noisy) hypersonic wind-tunnel environments. When these results were used, five separate design

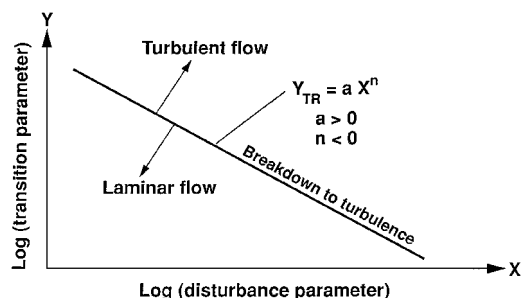


Fig. 1 Schematic of generalized correlation approach.

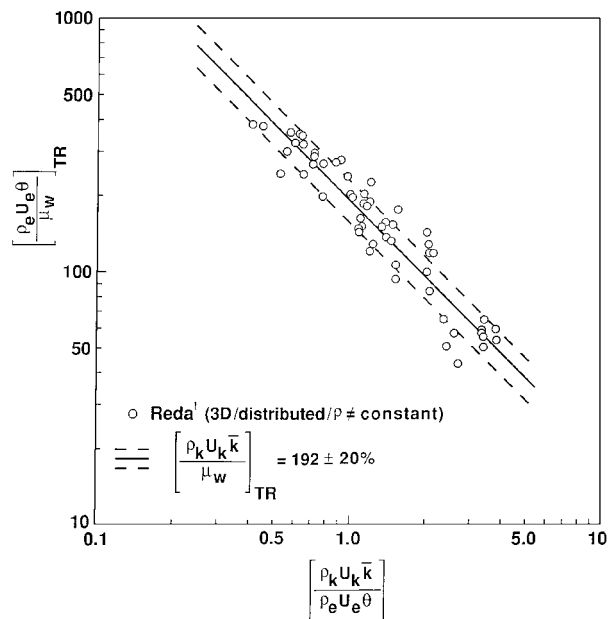


Fig. 2 Nosetip transition data from ballistics-range experiments; three-dimensional distributed roughness, compressible flows.

correlations were published, each claiming to model correctly the physics of transition onset and progression over actual nosetips undergoing reentry.¹

Figure 1, taken from Ref. 1, shows a schematic of the generalized correlation approach applied to the hypersonic wind-tunnel database.²¹ Power-law relationships between the assumed disturbance parameter X (based on the average surface roughness height) and the assumed transition parameter Y_{tr} (based on the computed, smooth-wall laminar boundary layer) were sought. In log-log coordinates, a correlation fitted with a -45 deg slope ($n = -1$) represented a unique situation where $Y_{tr} \cdot X = a = \text{const}$. At low X values, Y_{tr} values would asymptote (plateau) to a smooth-wall value that was a function of the noise level of the facility utilized, whereas at large X values, Y_{tr} values would asymptote (plateau) to a limiting value that could be interpreted one of two ways: Either the roughness had become large compared to the boundary-layer thickness, hence, further increases in roughness height had no additional effect on transition (the “protuberance” limit), or the unit Reynolds number had become low enough that roughness-induced disturbances, no matter how large, failed to amplify and died out.

Ballistics-range experiments, using laminar preablating nosetips of actual reentry materials, were subsequently conducted.¹ Analyses of this extensive real-materials/real-environments database showed that only one transition correlation, based on the concept of a critical roughness Reynolds number for transition, could successfully describe both the wind-tunnel and ballistics-range data sets, thus validating the application of this concept to actual reentry materials and conditions. Figure 2 shows a summary of the ballistics-range data set¹ for five different materials and three different nosetip radii exposed to quiescent, real-gas environments. This three-dimensional, distributed roughness data set was well represented by a critical roughness Reynolds number (based on conditions at the average roughness height and the wall temperature) of 192. The value

of this critical parameter for the three-dimensional, distributed roughness, wind-tunnel data set²¹ was lower (160), most probably due to additional disturbances imposed on the laminar boundary layer from nozzle-wall radiated noise and/or convected freestream disturbances.³ For both data sets, the computational methodology described by Dirling et al.¹⁹ and Dirling²⁰ was employed to calculate the smooth-wall laminar boundary-layer development and conditions at the average roughness height.

Demetriades,²² in his studies of the effects of three-dimensional distributed roughness on transition in the nozzle throat of a quiet supersonic wind tunnel, found corroborating evidence to support the ballistics-range result,¹ namely, a constant roughness Reynolds number for transition of 200 in the roughness-dominated regime. Note that a sonic-nozzle-throat flowfield closely simulates the flowfield over a blunt body in hypersonic flow, expanding from stagnation conditions, through Mach 1, to low supersonic Mach numbers.

Approximately two years after the present author's findings were published, Batt and Legner²³ published a review of the then available roughness-induced nosetip transition data sets.^{1,21,24} A thorough discussion was given of the difficulties and uncertainties in characterizing a three-dimensional ablated-surface microroughness pattern by a single height scale, generally chosen to be the average of the measured height distribution. An alternative height scale, the 30th-percentile probability-of-exceedance value, was chosen as being more representative of the disturbance-generation capability of any given laminar-ablated surface. Whereas this assumption may, in fact, be justifiable, Batt and Legner²³ incorrectly applied the Dirling transformation²⁵ in their subsequent analyses²³ of available surface microroughness distributions. This mathematical transformation allows the average in-plane roughness height, measured on a cross-sectional plane of an ablated sample via microscopy, to be converted to its corresponding average three-dimensional roughness element height once a geometrical shape for the elements, for example, spherical or conical, has been assumed. This transformation cannot be applied to any arbitrary value within the measured in-plane roughness-height distribution. The end result of their analysis was a conclusion counter to that reached in Ref. 1 and corroborated in Ref. 22: A modified-PANT transition correlation was offered as the correct model for transition onset/progression on roughened nosetips in hypersonic flows. Figures 8 and 10 of Ref. 23 show, however, that the uncertainty (scatter) bands on the dependent variable (the transition parameter) in these modified-PANT correlations are excessively large, ranging from +75 to -42% about the correlation fit in both cases. Despite such large uncertainties, modified-PANT transition correlations^{23,26} were applied by the reentry community of the 1980s, perhaps as a result of their ease of usage; only calculations of boundary-layer edge and integral parameters were required, as opposed to the more detailed computations of smooth-wall laminar boundary-layer density, velocity, and temperature profiles required by the critical roughness Reynolds number approach. Note, however, that the authors of Ref. 23 stated "A physical rationale for the (modified-PANT) correlation can be obtained by appealing to the critical Reynolds number approach."

In closing this section, it is emphasized again that roughness Reynolds numbers should be evaluated based on conditions in the smooth-wall laminar boundary layer at the roughness height, Re_{kk} . (Note that under adiabatic or near-adiabatic wall conditions, $\mu_w \cong \mu_k$; also, for small roughness, the elements can be assumed to be at the wall temperature.) Correlations to be discussed in subsequent sections were formulated and presented as graphical or algebraic representations of transition data sets and were based on smooth-wall laminar boundary-layer edge conditions. In most cases, insufficient information was available to allow the conversion of published results into Reynolds number Re_{kk} values. Hence, for purposes of comparison and discussion, Fig. 3 shows the ballistics-range database of Fig. 2 replotted in coordinates that allow the definition of $Re_{ke} = 106$.

Sensitivity of Correlation Approach to Computational Methods

In the time frame of the 1970s, smooth-wall laminar boundary-layer development was calculated via separate/iterative solutions

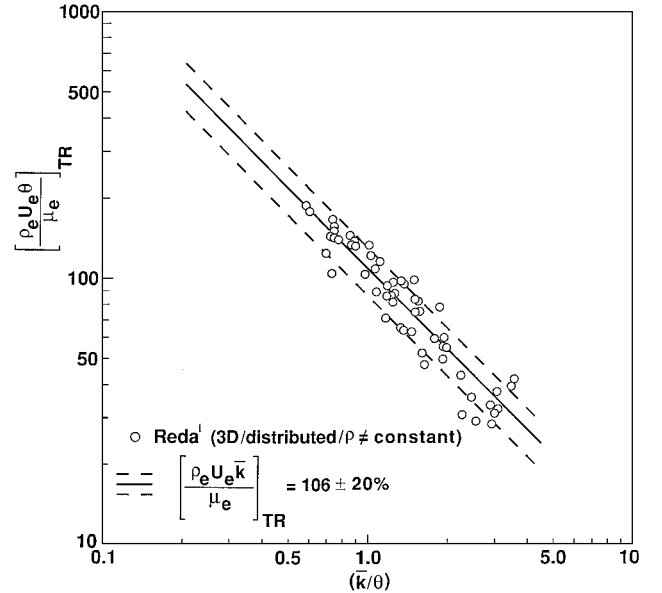


Fig. 3 Nosetip transition data from ballistics-range experiments; three-dimensional distributed roughness, compressible flows.

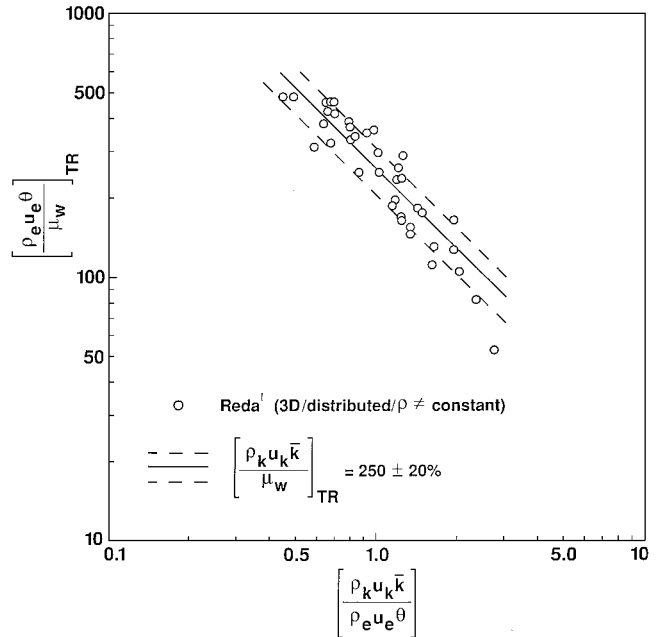


Fig. 4 Graphite nosetip transition data from ballistics-range experiments, analyzed using real-gas Navier-Stokes code; three-dimensional distributed roughness, compressible flows.

for the inviscid and viscous portions of the overall flowfield.^{19,20} Present-day, real-gas, Navier-Stokes codes (see Ref. 27) allow the entire viscous/inviscid flowfield to be calculated in a direct and, presumably, more accurate manner.

The graphite nosetip database of Ref. 1 was reanalyzed by Olejniczak of NASA Ames Research Center using the real-gas Navier-Stokes code described in Ref. 27. Results are shown in Fig. 4. Edge conditions predicted by the Dirling methodology^{19,20} and the Navier-Stokes methodology (see Ref. 27) were found to be in excellent agreement. More important, the critical roughness Reynolds number correlating approach was proven to remain valid, that is, a slope of $n = -1$ and an uncertainty band of $\pm 20\%$ were found to well represent the database. However, the value of the critical roughness Reynolds number was found to be approximately 25% higher when using the Navier-Stokes code to predict the smooth-wall laminar boundary-layer development, that is, a value of ~ 200 increased to ~ 250 . More detailed comparisons between

available present-day codes²⁸ need to be done to quantify further the sensitivity of this correlation approach to the choice of computational methods and thermophysical models.

Attachment Lines

During the past two decades, the influence of isolated roughness elements on swept-cylinder attachment-line boundary-layer transition was studied by Poll^{29,30} and Flynn and Jones.³¹ Although these experiments were conducted in incompressible flows, results are relevant to attachment-line transition physics for lifting-entry vehicles. Although these authors did acknowledge the roughness Reynolds number correlating approach, transition results were graphically presented in terms of Poll's disturbance parameter^{29,30} k/η (roughness height nondimensionalized by a computed length scale) and transition parameter \bar{R} (a Reynolds number based on edge conditions and the same computed length scale), that is, (k/η) is the disturbance parameter and \bar{R}_{tr} is the transition parameter, where

$$\bar{R} = \frac{\rho_e V_e \eta}{\mu_e} \quad (1)$$

$$\eta = \left[\frac{v_e}{(dU_e/dx)_{al}} \right]^{\frac{1}{2}} \quad (2)$$

Plots of their effective-tripping data sets in log-log coordinates (Figs. 5 and 6) showed an inverse dependence between the disturbance parameter and the transition parameter:

$$\bar{R}_{tr} = C[k/\eta]^{-1} \quad (3)$$

$$[\rho_e V_e \eta / \mu_e]_{tr} \cdot [k/\eta] = C \quad (4)$$

$$[\rho_e V_e k / \mu_e]_{tr} = C \cong 800 \text{ (two-dimensional, isolated)} \quad (5)$$

The end result is that the computed length scale cancels out, yielding a critical roughness Reynolds number (based on roughness height and boundary layer edge conditions) of 800 for two-dimensional isolated elements and 1000 for three-dimensional isolated elements.

Available compressible-flow attachment line transition onset data, for two-dimensional isolated roughness elements,^{32–36} are

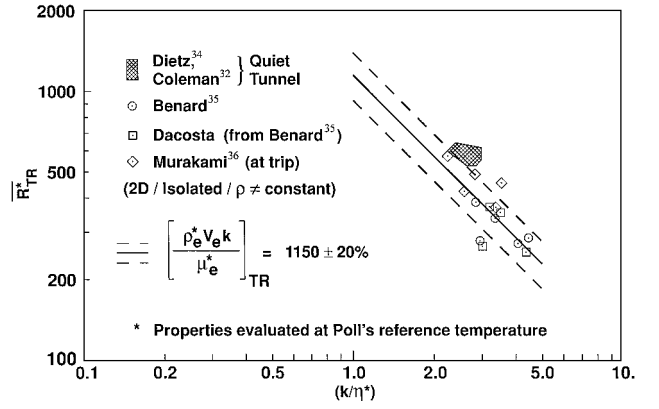


Fig. 7 Attachment line transition onset data from noisy and quiet wind-tunnel experiments; two-dimensional isolated roughness, compressible flows.

shown in Fig. 7 in terms of Poll's correlating parameters.^{29,30} Fluid properties are evaluated at Poll's reference temperature (see Ref. 35 for details). All models were swept cylinders.

Coleman^{32,33} and Dietz et al.³⁴ conducted experiments at a low freestream supersonic Mach number of 1.6 in a quiet facility. All other data shown were acquired in conventional (noisy) hypersonic facilities at freestream Mach numbers ranging from 5 to 7. Except for the data of Murakami et al.,³⁶ all measured transition onset locations were downstream of the trip location, a slight departure from the effective-tripping (transition at the roughness element) methodology applied in Figs. 5 and 6. All but 3 of the 14 compressible-flow data points fall within the band corresponding to a critical roughness Reynolds number of $1150 \pm 20\%$. The low Mach number/quiet-facility data all fall along the upper boundary of the noisy-facility results.

Lifting-Entry Vehicles

The pioneering research of Bertin et al.³⁷ and Goodrich et al.^{38,39} conducted in the early 1980s provided the basis for the understanding and modeling of transition onset and progression over the windward surface of the Space Shuttle Orbiter during reentry. Figure 8 shows $Re_{kk,tr}$ vs $(X/L)_{tr}$ measured on the shuttle windward centerline during actual reentry of STS-1–STS-5.³⁹ The three-dimensional, distributed surface roughness pattern due to TPS tile misalignments had an average height scale of 0.06 in. The basic thesis of the present paper is, once again, corroborated: For axial locations along the windward-surface centerline downstream of the nose-induced, favorable pressure-gradient region, $0.2 \leq (X/L)_{tr} \leq 1.0$, transition onset and progression were well modeled by an average critical roughness Reynolds number of 121. (Note that the stabilizing influence of such local, favorable pressure gradients on isolated-roughness-induced disturbances was reported earlier by Morrisette.⁴⁰) Figure 9 shows corresponding data bands measured in conventional (noisy) hypersonic wind tunnels.³⁹ Consistent with observations made previously, transition in the presence of both distributed roughness and radiated noise tends to occur earlier (lower Reynolds number $Re_{kk,tr}$ values) when compared to data obtained in quiet ground-based facilities or in-flight.

Between the lifting-entry-vehicle transition research of the early 1980s^{37–39} and that of the late 1990s,^{41–43} utilization of the critical roughness Reynolds number correlation approach waned. Berry et al.^{42,43} investigated the influence of isolated three-dimensional roughness elements on boundary-layer transition for hypersonic flows over both the Space Shuttle Orbiter and X-33 configurations at high angles of attack. Based on these results, an algebraic correlation was given between the postulated disturbance parameter k/δ (roughness height nondimensionalized by smooth-wall laminar boundary-layer thickness) and the postulated transition parameter Re_θ/M_e (edge Reynolds number, based on smooth-wall laminar boundary-layer momentum thickness, divided by edge Mach number), that is, (k/δ) is the disturbance parameter and $(Re_\theta/M_e)_{tr}$ is the transition parameter:

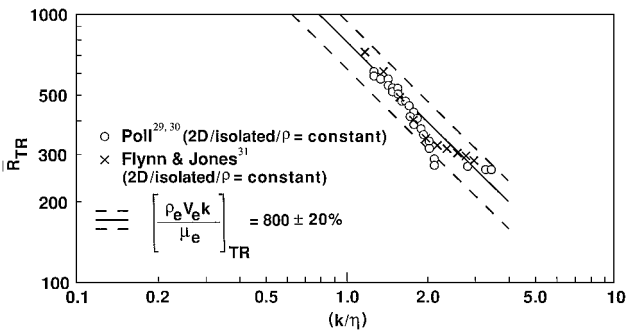


Fig. 5 Attachment line transition correlation based on wind-tunnel experiments; two-dimensional isolated roughness, incompressible flows.

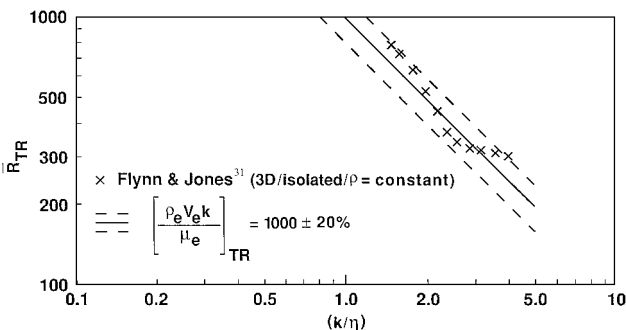


Fig. 6 Attachment line transition correlation based on wind-tunnel experiments; three-dimensional isolated roughness, incompressible flows.

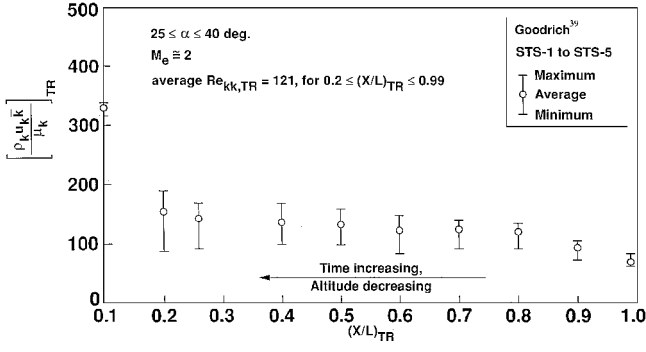


Fig. 8 Transition onset and progression for space shuttle centerline; reentry data, three-dimensional distributed roughness, compressible flows.

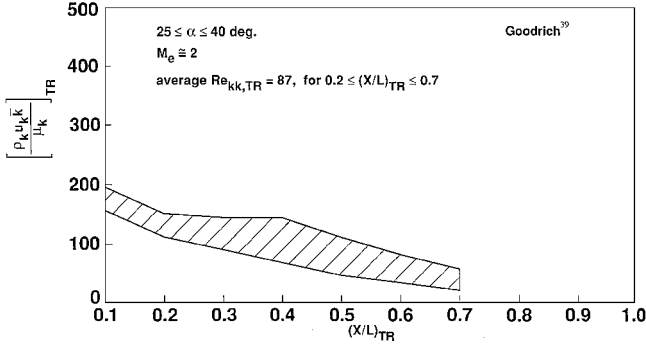


Fig. 9 Transition onset and progression for space shuttle centerline; wind-tunnel experiments, three-dimensional distributed roughness, compressible flows.

$$(Re_\theta / M_e)_\text{tr} = C(k/\delta)^{-1} \quad (6)$$

Algebraic manipulation of Eq. (6) leads to

$$[\rho_e U_e k / \mu_e]_\text{tr} = C \cdot M_e \cdot (\delta/\theta) \quad (7)$$

For high-angle-of-attack hypersonic flows about flat-bottomed lifting-entry vehicles, both M_e and (δ/θ) for laminar boundary layers are essentially constant parameters. Thus, Eq. (7) says that the algebraic correlations of Refs. 42 and 43 are equivalent to stating that there is a critical roughness Reynolds number for transition on such vehicles due to three-dimensional isolated roughness elements. To estimate the value of this critical parameter for both the shuttle and X-33, we choose $M_e = 2$ and $(\delta/\theta) = 7.5$ (the incompressible limit) as representative values. The product of M_e and (δ/θ) assumed here is, thus, 15; corresponding values of this product taken from Table 2 of Bouslog et al.⁴¹ for the Space Shuttle Orbiter geometry range from 11.06 to 19.31, with an average value of 15.39. The value for the constant C in each case was determined from a log-log correlation plot using the coordinates of the algebraic correlation.

Figure 10 shows the shuttle windward centerline data of Ref. 42 replotted in log-log coordinates, consistent with the generalized correlation approach of Fig. 1. This isolated roughness data set is well fitted by

$$[\rho_e U_e k / \mu_e]_\text{tr} = 450 \pm 20\% \quad (8)$$

Figure 11 shows the same data set replotted in the coordinates used in Fig. 2. Table 2 of Bouslog et al.⁴¹ was used to provide the required information concerning conditions in the smooth-wall laminar boundary layer at the roughness height. Except for the two lowest disturbance parameter data points, this isolated roughness data set is well fitted by

$$[\rho_k U_k k / \mu_w]_\text{tr} = 344 \pm 20\% \quad (9)$$

Note again that as the disturbance parameter based on k is systematically reduced in such experiments the transition parameter

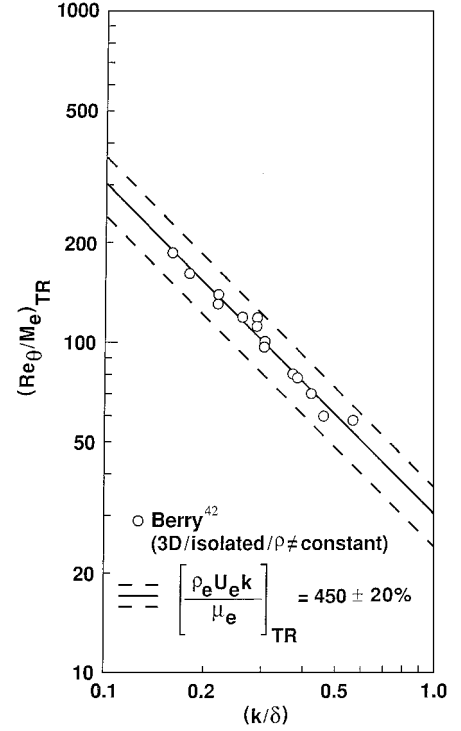


Fig. 10 Transition data for space shuttle centerline; wind-tunnel experiments, three-dimensional isolated roughness, compressible flows.

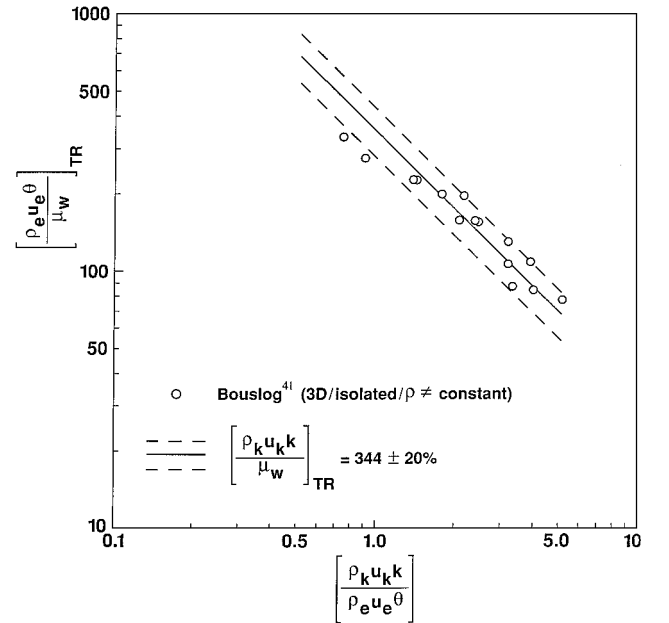


Fig. 11 Transition data for space shuttle centerline; wind-tunnel experiments, three-dimensional isolated roughness, compressible flows.

asymptotes or plateaus to a smooth-wall limit dictated by the disturbance level (radiated noise and/or freestream turbulence) of the facility utilized.

Figures 12 and 13 show the three-dimensional, isolated-roughness transition data sets for the X-33 centerline and attachment line, respectively.⁴³ The same analysis approach used in Fig. 10 is applied here. Both data sets are well represented by

$$[\rho_e U_e k / \mu_e]_\text{tr} = 1050 \pm 20\% \quad (10)$$

When based on edge conditions, this critical roughness Reynolds number for three-dimensional isolated roughness in compressible flows agrees quite well with the corresponding value of Flynn and Jones³¹ for incompressible attachment-line flows (see again Fig. 6).

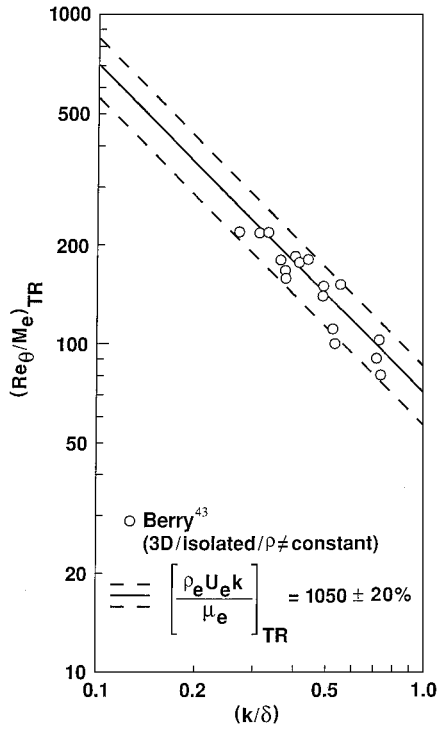


Fig. 12 Transition data for X-33 centerline; wind-tunnel experiments, three-dimensional isolated roughness, compressible flows.

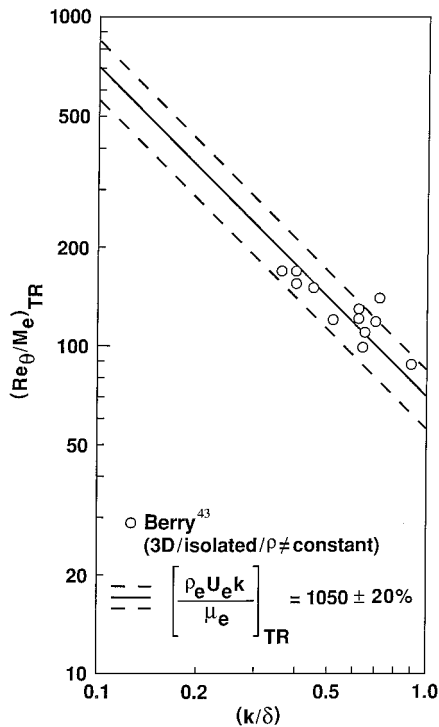


Fig. 13 Transition data for X-33 attachment line; wind-tunnel experiments, three-dimensional isolated roughness, compressible flows.

Insufficient information was given to recast the X-33 data into Reynolds number $Re_{kk, tr}$ values.

One final note concerning the X-33 results warrants discussion. Initial results were reported in Ref. 43 concerning the effects of three-dimensional distributed roughness on windward-surface transition. The roughness pattern was chosen to simulate metallic-panel bowing due to thermal distortion, but the pattern was applied only to the upstream third or so of the windward surface. Dome heights ranged from 0.002 to 0.008 in., and the wavelength of the pattern was large compared to its amplitude. The resultant surface pattern

in each simulation was a wavy wall that did not have the multiple height scales (back steps, edge ripples, and dome heights) typically attributed to such heat-shield designs. The thermal phosphor coating used to detect transition was applied over the wavy-wall pattern, reducing the effective dome heights by an unreported amount. The tripping effectiveness of such wavy-wall patterns was found to be slightly less than that of isolated roughness elements of comparable height scales, in apparent contradiction to present understanding.

Design Implications

When the isolated-roughness data listed in Table 2 of Bouslog et al.⁴¹ and the distributed-roughness data reported by Goodrich et al.³⁹ are referred to, a comparison of ground-based (noisy) transition data measured on the shuttle centerline shows that

$$\frac{Re_{kk, tr} \text{ (three-dimensional, isolated)}}{Re_{kk, tr} \text{ (three-dimensional, distributed)}} = \frac{344}{87} \approx \frac{4}{1} \quad (11)$$

Further, if one ignores noise and configuration effects, a worst-case comparison of Figs. 3 and 12 shows

$$\frac{Re_{ke, tr} \text{ (three-dimensional, isolated)}}{Re_{ke, tr} \text{ (three-dimensional, distributed)}} = \frac{1050}{106} \approx \frac{10}{1} \quad (12)$$

Ratios (11) and (12) clearly indicate that transition occurs earlier (at lower critical roughness Reynolds numbers) for flows over distributed-surface-roughness patterns as compared to isolated-roughness cases. The X-33 flight test vehicle was designed⁴⁴ based on the isolated-roughness correlation of Eq. (6), and hence, its transition performance might well have been outside the design envelope. It now appears, however, that this vehicle will never be flown.

As noted in the Introduction, designs proposed for future reusable launch vehicles will employ metallic-panel, nonablating TPS. The windward surface of such a vehicle will comprise overlapping, sharp-cornered, metallic panels yielding a periodic distributed array of steps with edges skewed to local flow directions (see Fig. 1 of Ref. 45). To complicate matters further, computations and arc-jet tests indicate that such metallic panels bow under reentry heating and that the edges ripple to form a quasi-periodic distributed-surface-roughness pattern of multiple height scales.⁴⁵ For such heat shields, transition onset could potentially occur at altitudes significantly higher than anticipated, and turbulence could potentially progress forward over the windward surface more rapidly than anticipated, resulting in higher heat transfer rates for long times. Viable designs will, thus, require a better understanding of the tripping effectiveness of such thermally induced distributed-surface-roughness patterns.

Conclusions

1) Based on analyses of existing roughness-dominated transition correlations for blunt bodies, attachment lines, and windward surfaces of lifting-entry vehicles, it was found that all such correlations could be well modeled by the critical roughness Reynolds number concept.

2) Three-dimensional, distributed-surface-roughness patterns promote earlier transition as compared to the tripping effectiveness of a single, three-dimensional roughness element of equivalent height and shape. Available data sets indicate that critical roughness Reynolds numbers, for flows over three-dimensional distributed-roughness patterns, can be factors of 4–10 times less than corresponding values measured for three-dimensional isolated-roughness cases.

3) Because there are an infinite number of potential flowfields, that is, combinations of geometries, approach flows, and boundary conditions, within which laminar boundary layers can develop, and there are an infinite number of potential surface roughness patterns, no universal value for the critical roughness Reynolds number for transition to turbulence exists. The critical value for any flow-field/roughness pattern combination must be determined empirically in a quiet ground-based test facility or in-flight.

4) Empirical determination of a critical value for a specific subset of flows, namely, three-dimensional distributed roughness on hemispheres in hypersonic flows, has been successfully demonstrated in quiescent ballistics-range environments.

References

- ¹Reda, D. C., "Correlation of Nosedip Boundary-Layer Transition Data Measured in Ballistics-Range Experiments," *AIAA Journal*, Vol. 19, No. 3, 1981, pp. 329-339.
- ²Schneider, S. P., "Flight Data for Boundary-Layer Transition at Hypersonic and Supersonic Speeds," *Journal of Spacecraft and Rockets*, Vol. 36, No. 1, 1999, pp. 8-20.
- ³Schneider, S. P., "Effects of High-Speed Tunnel Noise on Laminar-Turbulent Transition," *Journal of Spacecraft and Rockets*, Vol. 38, No. 3, 2001, pp. 323-333.
- ⁴Schiller, L., "Flow in Pipes," *Handbook of Experimental Physics*, Vol. 4, Pt. 4, Academic Press, Leipzig, Germany, 1932, pp. 189-192.
- ⁵Dryden, H. L., "Review of Published Data on the Effect of Roughness on Transition from Laminar to Turbulent Flow," *Journal of the Aeronautical Sciences*, Vol. 20, No. 7, 1953, pp. 477-482.
- ⁶Klebanoff, P. S., Schubauer, G. B., and Tidstrom, K. D., "Measurements of the Effect of Two-Dimensional and Three-Dimensional Roughness Elements on Boundary-Layer Transition," *Journal of the Aeronautical Sciences*, Vol. 22, No. 11, 1955, pp. 803, 804.
- ⁷Smith, A. M. O., and Clutter, D. W., "The Smallest Height of Roughness Capable of Affecting Boundary Layer Transition," *Journal of the Aero/Space Sciences*, Vol. 26, No. 4, 1959, pp. 229-245, 256.
- ⁸Braslow, A. L., Knox, E. C., and Horton, E. A., "Effect of Distributed Three-Dimensional Roughness and Surface Cooling on Boundary-Layer Transition and Lateral Spread of Turbulence at Supersonic Speeds," NASA TN D-53, Oct. 1959.
- ⁹Tani, I., "Effect of Two-Dimensional and Isolated Roughness on Laminar Flow," *Boundary Layer and Flow Control, Its Principles and Application*, edited by G. V. Lachmann, Vol. 2, Pergamon, New York, 1961, pp. 637-656.
- ¹⁰von Doenhoff, A. E., and Braslow, A. L., "The Effect of Distributed Surface Roughness on Laminar Flow," *Boundary Layer and Flow Control, Its Principles and Application*, edited by G. V. Lachmann, Vol. 2, Pergamon, New York, 1961, pp. 657-681.
- ¹¹Potter, J. L., and Whitfield, J. D., "Effects of Slight Nose Bluntness and Roughness on Boundary-Layer Transition in Supersonic Flows," *Journal of Fluid Mechanics*, Vol. 12, Pt. 4, 1962, pp. 501-535.
- ¹²Braslow, A. L., "A Review of Factors Affecting Boundary-Layer Transition," NASA TN D-3384, Aug. 1966.
- ¹³van Driest, E. R., and Blumer, C. B., "Boundary-Layer Transition at Supersonic Speeds: Roughness Effects with Heat Transfer," *AIAA Journal*, Vol. 6, No. 4, 1968, pp. 603-607.
- ¹⁴Gibbings, J. C., and Hall, D. J., "Criterion for Tolerable Roughness in a Laminar Boundary Layer," *Journal of Aircraft*, Vol. 6, No. 2, 1969, pp. 171-173.
- ¹⁵Tani, I., "Boundary-Layer Transition," *Annual Review of Fluid Mechanics*, edited by W. R. Sears and M. Van Dyke, Vol. 1, 1969, pp. 169-196.
- ¹⁶Reshotko, E., and Leventhal, L., "Preliminary Experimental Study of Disturbances in a Laminar Boundary Layer Due to Distributed Surface Roughness," AIAA Paper 81-1224, June 1981.
- ¹⁷Reshotko, E., "Disturbances in a Laminar Boundary Layer Due to Distributed Surface Roughness," *Turbulence and Chaotic Phenomena in Fluids*, edited by T. Tatsumi, Elsevier Science, Amsterdam, 1984, pp. 39-46.
- ¹⁸Tadjfar, M., Reshotko, E., Dybbs, A., and Edwards, R. V., "Velocity Measurements Within Boundary Layer Roughness Using Index Matching," *International Symposium on Laser Anemometry*, ASME FED, edited by A. Dybbs and P. A. Pfund, Vol. 33, American Society of Mechanical Engineers, Fairfield, NJ, 1985, pp. 59-73.
- ¹⁹Dirling, R. B., Jr., Swain, C. E., and Stokes, T. R., "The Effect of Transition and Boundary Layer Development on Hypersonic Reentry Shape Change," AIAA Paper 75-673, May 1975.
- ²⁰Dirling, R. B., Jr., "Asymmetric Nosedip Shape Change During Atmospheric Entry," *Aerodynamic Heating and Thermal Protection Systems*, edited by L. S. Fletcher, Vol. 59, Progress in Astronautics and Aeronautics AIAA, New York, 1978, pp. 311-327; also AIAA Paper 77-779, June 1977.
- ²¹Anderson, A. D., "Passive Nosedip Technology (PANT) Program, Interim Report, Volume X, Appendix A: Boundary Layer Transition on Nosedips with Rough Surfaces," Aerotherm Corp., Space and Missiles Systems Organization Rept. SAMSO-TR-74-86, Mountain View, CA, Jan. 1975.
- ²²Demetriades, A., "Roughness Effects on Boundary-Layer Transition in a Nozzle Throat," *AIAA Journal*, Vol. 19, No. 3, 1981, pp. 282-289.
- ²³Batt, R. G., and Legner, H. H., "A Review of Roughness-Induced Nosedip Transition," *AIAA Journal*, Vol. 21, No. 1, 1983, pp. 7-22.
- ²⁴Wassel, T., and Shih, W., "Roughness Induced Transition and Heat Transfer Augmentation in Hypersonic Environments," AIAA Paper 84-0631, March 1984.
- ²⁵Dirling, R. B., Jr., "On the Relation Between Material Variability and Surface Roughness," AIAA Paper 77-402, March 1977.
- ²⁶Chen, K. K., and Thyson, N., "Nosedip Shape Change Regimes: Laminar Boundary Layer with Roughness," Avco Systems Div., Space and Missiles Systems Organization, Rept. SAMSO-TR-75-269, Wilmington, MA, June 1976.
- ²⁷Wright, M. J., Candler, G. V., and Bose, D., "Data-Parallel Line Relaxation Method for the Navier-Stokes Equations," *AIAA Journal*, Vol. 36, No. 9, 1998, pp. 1603-1609.
- ²⁸Gnoffo, P. A., Weilmuenster, K. J., Hamilton, H. H., II, Olynick, D. R., and Venkatapathy, E., "Computational Aerothermodynamic Design Issues for Hypersonic Vehicles," *Journal of Spacecraft and Rockets*, Vol. 36, No. 1, 1999, pp. 21-43.
- ²⁹Poll, D. I. A., "Transition in the Infinite Swept Attachment Line Boundary Layer," *Aeronautical Quarterly*, Vol. 30, Pt. 4, 1979, pp. 607-629.
- ³⁰Poll, D. I. A., "The Effect of Isolated Roughness Elements on Transition in Attachment-Line Flows," *Laminar-Turbulent Transition*, edited by D. Arnal and R. Michel, Springer-Verlag, New York, 1990, pp. 657-667.
- ³¹Flynn, G. A., and Jones, R. I., "Attachment Line Transition with Three-Dimensional Isolated Roughness Elements," AIAA Paper 99-1018, Jan. 1999.
- ³²Coleman, C. P., "Boundary Layer Transition in the Leading Edge Region of a Swept Cylinder in High Speed Flow," NASA TM-112224, March 1998.
- ³³Coleman, C. P., and Poll, D. I. A., "Roughness-Induced Attachment-Line Transition on a Swept Cylinder in Supersonic Flow," *AIAA Journal*, Vol. 39, No. 4, 2001, pp. 590-596.
- ³⁴Dietz, A. J., Coleman, C. P., Laub, J. A., and Poll, D. I. A., "Effect of Wall Temperature on Roughness Induced Attachment-Line Transition," *Laminar-Turbulent Transition*, edited by H. F. Fasel and W. S. Saric, Springer-Verlag, New York, 2000, pp. 249-254.
- ³⁵Benard, E., Gaillard, L., and Alziary de Roquefort, T., "Influence of Roughness on Attachment Line Boundary Layer Transition in Hypersonic Flow," *Experiments in Fluids*, Vol. 22, No. 4, 1997, pp. 286-291.
- ³⁶Murakami, A., Stanewsky, E., and Krogmann, P., "Boundary-Layer Transition on Swept Cylinders at Hypersonic Speeds," *AIAA Journal*, Vol. 34, No. 4, 1996, pp. 649-654.
- ³⁷Bertin, J. J., Hayden, T. E., and Goodrich, W. D., "Shuttle Boundary-Layer Transition Due to Distributed Roughness and Surface Cooling," *Journal of Spacecraft and Rockets*, Vol. 19, No. 5, 1982, pp. 389-396.
- ³⁸Goodrich, W. D., Derry, S. M., and Bertin, J. J., "Shuttle Orbiter Boundary-Layer Transition: A Comparison of Flight and Wind Tunnel Data," AIAA Paper 83-0485, Jan. 1983.
- ³⁹Goodrich, W. D., Derry, S. M., and Bertin, J. J., "Shuttle Orbiter Boundary Layer Transition at Flight and Wind Tunnel Conditions," *Shuttle Performance: Lessons Learned*, NASA CP-2283, Pt. 2, 1983, pp. 753-779.
- ⁴⁰Morrisette, E. L., "Roughness Induced Transition Criteria for Space Shuttle-Type Vehicles," *Journal of Spacecraft and Rockets*, Vol. 13, No. 2, 1976, pp. 118-120.
- ⁴¹Bouslog, S. A., Bertin, J. J., Berry, S. A., and Caram, J. M., "Isolated Roughness Induced Boundary-Layer Transition: Shuttle Orbiter Ground Tests and Flight Experience," AIAA Paper 97-0274, Jan. 1997.
- ⁴²Berry, S. A., Bouslog, S. A., Brauckmann, G. J., and Caram, J. M., "Shuttle Orbiter Experimental Boundary-Layer Transition Results with Isolated Roughness," *Journal of Spacecraft and Rockets*, Vol. 35, No. 3, 1998, pp. 241-248.
- ⁴³Berry, S. A., Horvath, T. J., Hollis, B. R., Thompson, R. A., and Hamilton, H. H., II, "X-33 Hypersonic Boundary Layer Transition," *Journal of Spacecraft and Rockets*, Vol. 38, No. 5, 2001, pp. 646-657.
- ⁴⁴Thompson, R. A., Hamilton, H. H., II, Berry, S. A., Horvath, T. J., and Nowak, R. J., "Hypersonic Boundary-Layer Transition for X-33 Phase II Vehicle," AIAA Paper 98-0867, Jan. 1998.
- ⁴⁵Palmer, G., Kontinos, D., and Sherman, B., "Surface Heating Effects of X-33 Vehicle Thermal-Protection-System Panel Bowing," *Journal of Spacecraft and Rockets*, Vol. 36, No. 6, 1999, pp. 836-841.

T. C. Lin
Associate Editor